Molecules and Cells

Interaction of the Lysophospholipase PNPLA7 with Lipid Droplets through the Catalytic Region

Pingan Chang[1,*], Tengteng Sun[1], Christoph Heier[2], Hao Gao[1], Hongmei Xu[1], and Feifei Huang[1]

[1]Chongqing Key Laboratory of Big Data for Bio-intelligence, School of Bio-information, Chongqing University of Posts and Telecommunications, Chongqing 400065, China, [2]Institute of Molecular Biosciences, University of Graz, 8010 Graz, Austria
*Correspondence: changpa@cqupt.edu.cn
https://doi.org/10.14348/molcells.2020.2283
www.molcells.org

Mammalian patatin-like phospholipase domain containing proteins (PNPLAs) play critical roles in triglyceride hydrolysis, phospholipids metabolism, and lipid droplet (LD) homeostasis. PNPLA7 is a lysophosphatidylcholine hydrolase anchored on the endoplasmic reticulum which associates with LDs through its catalytic region (PNPLA7-C) in response to increased cyclic nucleotide levels. However, the interaction of PNPLA7 with LDs through its catalytic region is unknown. Herein, we demonstrate that PNPLA7-C localizes to the mature LDs *ex vivo* and also colocalizes with pre-existing LDs. Localization of PNPLA7-C with LDs induces LDs clustering via non-enzymatic intermolecular associations, while PNPLA7 alone does not induce LD clustering. Residues 742-1016 contains four putative transmembrane domains which act as a LD targeting motif and are required for the localization of PNPLA7-C to LDs. Furthermore, the N-terminal flanking region of the LD targeting motif, residues 681-741, contributes to the LD targeting, whereas the C-terminal flanking region (1169-1326) has an anti-LD targeting effect. Interestingly, the LD targeting motif does not exhibit lysophosphatidylcholine hydrolase activity even though it associates with LDs phospholipid membranes. These findings characterize the specific functional domains of PNPLA7 mediating subcellular positioning and interactions with LDs, as wells as providing critical insights into the structure of this evolutionarily conserved phospholipid-metabolizing enzyme family.

Keywords: lipid droplet, lysophosphatidylcholine hydrolase, PNPLA7, transmembrane domain

INTRODUCTION

As evolutionarily conserved organelles that store triacylglycerols (TAG) and sterol esters, lipid droplets (LDs) are surrounded by a phospholipid monolayer that associates with a wide variety of proteins (Barneda and Christian, 2017; Farese and Walther, 2009; Fujimoto and Parton, 2011). LDs are important dynamic organelles that respond to metabolic states and nutrient conditions (Reue, 2011). LD-associated proteins play critical roles in the formation and breakdown of LDs. Tens to hundreds of LD-associated proteins have been identified through proteomic experiments (Zhang and Liu, 2019). Common among them are perilipins in mammalian cells, which are involved in TAG synthesis and the breakdown of LDs which regulates their size and number (Sztalryd and Brasaemle, 2017).

Recently, the mammalian patatin-like phospholipase domain containing protein (PNPLA) family has attracted attention because many of its members have critical roles in energy metabolism, skin barrier development, and neuronal integrity (Kienesberger et al., 2009; Pichery et al., 2017). Nine PNPLA proteins have been identified and exhibit hydrolase, transacylase, or acyltransferase activities with diverse lipid substrates such as phospholipids, acylglycerols, and retinoids

Received 20 November 2019; revised 28 January 2020; accepted 10 February 2020; published online 18 March, 2020

eISSN: 0219-1032

(Kienesberger et al., 2009). Mammalian PNPLAs have been divided into three subgroups (Kienesberger et al., 2009; Wilson et al., 2006). The first subgroup, termed the adiponutrin family, contains PNPLA1-5; among them PNPLA2 (adipose triglyceride lipase, ATGL), PNPLA3 (adiponutrin), and PNPLA5 (GS2-like protein) are constitutively associated with LDs (Murugesan et al., 2013). In addition, PNPLA1 is recruited to the LD membrane by α/β-hydrolase domain containing 5 (ABHD5) (Kien et al., 2018; Ohno et al., 2018). The second subfamily includes PNPLA6 and PNPLA7, which are usually termed neuropathy target esterase (NTE) and NTE-related esterase respectively. PNPLA8 and PNPLA9 constitute the third subgroup (Kienesberger et al., 2009; Wilson et al., 2006).

PNPLA6 and PNPLA7 have been remarkably conserved through evolution with orthologous proteins existing in yeast, nematodes, and flies (Lush et al., 1998). They share a highly conserved domain architecture that is comprised of an amino-terminal transmembrane domain (TMD), a regulatory (R) region with three predicted cyclic nucleotide monophosphate (cNMP)-binding domains (CBDs), and a carboxyl-terminal catalytic esterase (C) region that includes a patatin domain (Kienesberger et al., 2008; Li et al., 2003) (Fig. 1A). The N-terminus of PNPLA7 is present in the endoplasmic reticulum (ER) lumen, whereas the C-terminus is cytosolic (Heier et al., 2017). PNPLA6 and PNPLA7 localize to the ER via its N-terminal TMD, while the R-region contributes to ER targeting (Heier et al., 2017; Li et al., 2003). Except for the N-terminal TMD, most of PNPLA6 and PNPLA7, which contain R and C regions, are cytosolic (Heier et al., 2017; Li et al., 2003). PNPLA6 has potent phospholipase activity which deacylates membrane lipids such as phosphatidylcholine (PC) and lysophosphatidylcholine (LPC) (Quistad et al., 2003; Zaccheo et al., 2004). PNPLA7 is also a lysophospholipase which hydrolyzes several lysophospholipids as determined by *in vitro* studies (Kienesberger et al., 2008). We further found that PNPLA7 functions acts as a potent intracellular lysophospholipase that primarily hydrolyzes LPC, particularly the unsaturated species found in living cells (Heier et al., 2017). The C-terminal regions of PNPLA6 and PNPLA7 exhibit similar catalytic activity similar to full-length proteins (Atkins and Glynn, 2000; Heier et al., 2017; Li et al., 2003; van Tienhoven et al., 2002).

PNPLA6 is primarily expressed in the nervous system, particularly in the brain and spinal cord, and plays several critical roles in mammalian neural development and adult axon maintenance (Akassoglou et al., 2004; Read et al., 2009). PNPLA7 is expressed in testis and insulin target tissues such as skeletal muscle, heart, and adipose tissues where it regulates responses to feeding/fasting transitions and insulin concentrations (Chang et al., 2012; Kienesberger et al., 2008). Recently, PNPLA7 was found to associate with LDs upon elevated fatty acid fluxes (Heier et al., 2017; Kienesberger et al., 2008). Our previous study demonstrates that the interaction of PNPLA7 with LDs is dependent on its catalytic domain and promoted by increased cNMP levels, such as cAMP and cGMP (Heier et al., 2017). The expression, catalytic activity, and localization of PNPLA7 are closely linked to lipid metabolism and energy homeostasis.

How does PNPLA7 interact with LDs through its catalytic

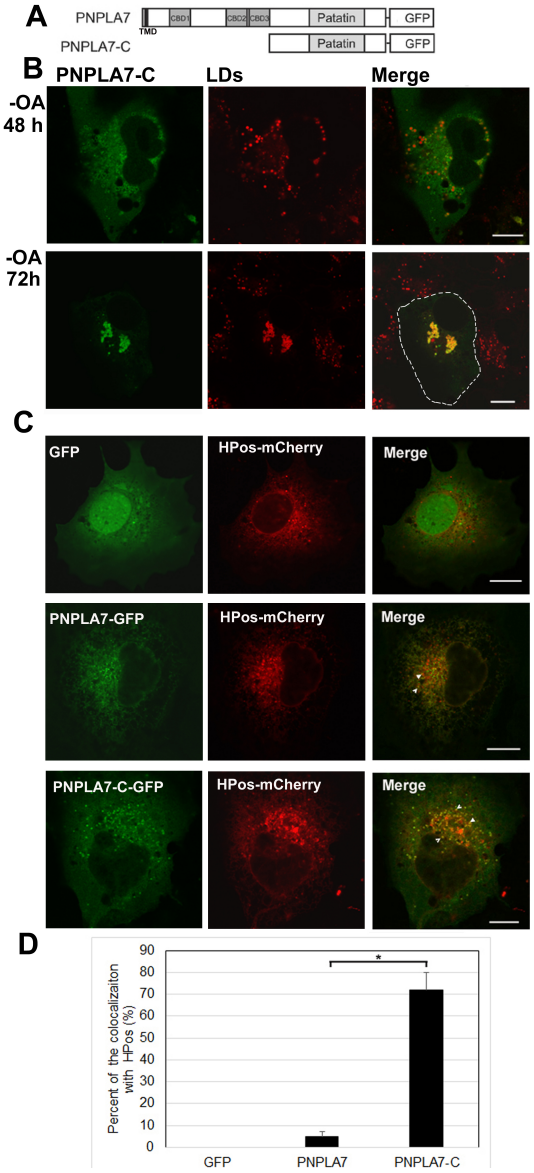

Fig. 1. PNPLA7-C localizes to LDs. (A) Domain architecture of PNPLA7 and PNPLA7-C. (B) PNPLA7-C-GFP localizes to LDs in a few of COS7 cells even without OA loading. At 48 h and 72 h post-transfection, COS7 cells were fixed and incubated with LipidTOX Red to stain LDs. Colocalization of PNPLA7-C and LDs was visualized by confocal laser scanning microscopy. The cell boundary was indicated by discontinuous short white lines. Scale bars = 10 μm. (C) PNPLA7-C colocalizes with the pre-LD marker HPos. COS7 cells co-expressing GFP, PNPLA7-C-GFP, or PNPLA7-GFP and HPos-mCherry were starved for 24 h. PNPLA7-C-GFP is present in HPos-positive puncta upon starvation, whereas PNPLA7 does not colocalize with pre-LDs stained by HPos-mCherry. White arrows indicate colocalization of proteins with pre-LDs marker HPos. Scale bars = 10 μm. (D) Quantification of the percentage of HPos-positive pre-LDs that accumulated in co-transfected proteins. Data are representative of three independent experiments and are expressed as means of total 50 cells. Error bars represent SD. Statistical significance was determined using Student's unpaired *t*-test. $*P < 0.05$.

region? There is no consensus as to how LD targeting motifs confer LD associations (Zhang and Liu, 2019). Even within the closely related members in the first PNPLA family subgroup, PNPLA2, PNPLA3 and PNPLA5 all employ different molecular motifs to interact with LDs (Murugesan et al., 2013). In addition, PNPLA7 belongs to the second PNPLA subfamily and has a different domain architecture when compared to other subgroups (Kienesberger et al., 2009; Wilson et al., 2006). Our previous results identified a stretch of 287 amino acids (681-967) mediates the interaction of PNPLA7 with LDs (Heier et al., 2017). In the current study, the interaction of PNPLA7 through its catalytic region with LDs is further explored to define the structural and functional domains that allow PNPLA7 to interact with LDs.

MATERIALS AND METHODS

Materials

African green monkey kidney fibroblast-like COS-7 cells were purchased from the Cell Center of Chinese Academy of Medical Sciences (China). PNPLA7-GFP, PNPLA7-ΔR-GFP, PNPLA7-C-GFP, PNPLA7-C2, C3, C4, C5, and C8 were constructed in our lab (Heier et al., 2017). The pGFP-HPos plasmid was gift from Prof. Albert Pol (Institut d'Investigacions Biomèdiques August Pi i Sunyer, Spain) (Kassan et al., 2013). Plasmid pEGFP-N3 and CAV1-mCherry were purchased from Clontech (USA) and Addgene (USA), respectively. Transfection reagents Lipofectamine 2000 and HCS LipidTOX Deep Red HCS LipidTOX Deep Red were obtained from Thermo Fisher Scientific (USA). Cell culture reagents and oleic acid (OA) were purchased from Sigma-Aldrich (USA). Q5 Site-Directed Mutagenesis Kit was purchased from New England Biolabs (USA). Pfu DNA polymerase, *Xho* I, *Eco*R I, and *Age* I were purchased from Takara (China). LPC (1-palmitoyl-sn-glycero-3-phosphocholine) and 8-CPT-cAMP were purchased from Sigma-Aldrich. Mouse anti-GFP, anti-GAPDH, anti-perilipin 2 (PLIN2) monoclonal antibodies, and goat anti-mouse IgG HRP were from Santa Cruz Biotechnology (USA). Enhanced chemiluminescence (ECL) reagents are obtained from Pierce Biotechnology (USA). NEFA-HR (2) kit was obtained from WAKO Chemicals GmbH (Germany).

Transmembrane domain analysis

TMDs in PNPLA7-C were predicted using TMHMM (Krogh et al., 2001), SOSUI (Hirokawa et al., 1998), TMpred (Hofmann and Stoffel, 1993), HMMTOP (Tusnády and Simon, 2001), and TopPred (Claros and von Heijne, 1994).

Plasmids construction

PNPLA7 truncation mutants were generated by polymerase chain reaction (PCR) using the primers shown in Table 1. The PCR products were purified by agarose gel electrophoresis and cloned into the multiple cloning site of pEGFP-N3 using the restriction sites for *Xho* I and *Eco*R I to create C-terminal in-frame fusions with GFP. The internal deletion mutant of PNPLA7-C for ΔTM (Δ742-1017) was generated using the Q5 Site-Directed Mutagenesis Kit with PNPLA7-C-GFP as template and primers indicated in Table 1. To construct PNPLA7-C13 and C14, PNPLA7-C2 and C8 were used as templates respectively and performed according to the Q5 Site-Directed Mutagenesis Kit manual. To generate a plasmid encoding HPos-mCherry, the cDNAs of HPos were amplified using the primers, 5'- GCGAATTCGCCATGGATGCCCTGGTTCTATT -3' and 5'- CAGGATCCCGTATCTCTTTCTGCGTGCTGA -3' using pGFP-HPos as a template (Kassan et al., 2013). The PCR products were digested with *Eco*R I and *Bam*H I and ligated into the multiple cloning site of pCAV1-mCherry. All plasmids were sequenced to confirm the presence of the desired mutations.

Cell culture, transfection, and treatment

COS-7 cells were cultured in Dulbecco's modified Eagle's medium (DMEM) with 10% fetal bovine serum in a 37°C incubator with 5% CO_2. Cell transfections were performed using Lipofectamine 2000 transfection reagent as per the manufacturer's directions. COS-7 cells were starved in DMEM in the absence of serum for 24 h directly after transfection of PNPLA7-GFP or PNPLA7-C-GFP with HPos-mCherry to observe the associations with pre-existing LDs. To stimulate TAG synthesis and LD formation, 24-h post-transfection, cells

Table 1. The Primers used to generate PNPLA7-C constructs

Construct name	Primer name	Primer sequence (5'-3')
PNPLA7-C9	TM1F	TTCTCGAGGCCATGTTTGCTCTGGAGCTCCAACA
	TM9R	GCGAATTCGAGAAGATGTTGCTGATGCTGC
PNPLA7-C10	TM2F	TTCTCGAGGCCATGCTGACAGGCAATGCCATT
	TM10R	GCGAATTCGAGAAGATGTTGCTGATGCTGC
PNPLA7-C11	TM1F	TTCTCGAGGCCATGTTTGCTCTGGAGCTCCAACA
	TM11R	GCGAATTCGACTCTAGGACACCACTCCGGA
PNPLA7-C12	TM1F	TTCTCGAGGCCATGTTTGCTCTGGAGCTCCAACA
	TM12R	GCGAATTCGACCTCAGGTACTCACAGTAGT
PNPLA7-C13	ΔTM2F	CAGGTGGGCATCCTCAGG
	ΔTM2R	CCGTGCCAGGCGGGAAAA
PNPLA7-C14	ΔTM2F	CAGGTGGGCATCCTCAGG
	ΔTM2R	CCGTGCCAGGCGGGAAAA
ΔTM-PNPLA7-C	NDTF	AAAGACCGGCAGATTGAGGAC
	NDTR	GGCGGTTAGGGGCACATC

were cultured in DMEM medium containing 400 μM OA complexed with fat-free bovine serum albumin (BSA) for 16 h. In order to enhance the association of PNPLA7 with LDs, cells were treated with 400 μM OA and 1 mM 8-CPT-cAMP for 16 h before being processed for imaging.

LDs purification

For LD isolation, cells were harvested, washed twice with PBS, and resuspended in cold lysis buffer A (20 mM Tris/HCl pH 7.4, 1 mMEDTA) containing freshly added protease inhibitors (1 mM sodium orthovanadate, 1 mMNaF, 1 μg/ml Leupeptin, 10 μg/ml Aprotinin, 1 mM PMSF), and then homogenized with a Dounce homogenizer on ice. LDs were isolated by a discontinuous sucrose gradient ultracentrifugation as described by Braesaml and Wolins with minor modifications (Brasaemle and Wolins, 2016). Protein concentrations of cell extracts were determined with the Bio-Rad Protein Assay Kit (Bio-Rad, USA) using BSA as standard.

Immunoblotting analysis

After transfection for 48 h, total protein samples were prepared by sonication in RIPA Buffer containing 20 μg/ml leupeptine, 2 μg/ml antipain, and 1 μg/ml pepstatin, and then centrifuged at 4°C and 15,000*g* for 15 min to pellet the cell debris. The supernatant was used to further immunoblotting analysis. The protein concentration was determined with Pierce BCA Protein Assay Kit (Pierce Biotechnology). The protein expression in total cell and LDs extracts were assayed by western blotting using anti-GFP antibodies (Huang et al., 2016). Blots were then stripped and re-probed for anti-GAPDH or anti-PLIN2 antibody.

LD staining and confocal fluorescence microscopy

COS-7 cells were seeded in chambers mounted onto cover slips (Sarstedt, Germany) and transfected as described above. After transfection for the indicated time, the cells are washed three times with 1× PBS and then fixed with 4% paraformaldehyde (PFA) for 20 min at room temperature. For detection of protein and LD colocalization, LDs were stained by incubating the cells with HCS LipidTOX Red Neutral Lipid stain (1:500 in PBS) for 30 min. Fluorescent images were acquired by confocal scanning microscopy with a Leica SP5 confocal microscope equipped with a Leica HCX 63×1.4 NA oil immersion objective. Enhanced GFP was excited at 488 nm and emission was detected between 500 and 530 nm. mCherry was excited at 561 nm and emission was detected between 580 and 610 nm. HCS LipidTOX Deep Red was excited at 633 nm and emission was detected between 650 and 700 nm. All the presented experiments are repeated independently at least three times.

LD quantification

The percentage of the HPos-positive pre-LDs were quantified as previously described (Kassan et al., 2013). In brief, transfected cells were selected randomly. For each experiment, images were captured under the same conditions. All images were single confocal sections and analyzed with Photoshop CS software (Adobe, USA). The quantification of number of pre-LDs, and the colocalization of transfected proteins with HPos were performed in three independent experiments and at least 50 cells per experiment were acquired using ImageJ software (National Institutes of Health, USA). LDs were classified as clustered, intermediate, and dispersed as previously described (Papadopoulos et al., 2015). When more than 50% of the LDs were clustered on one side of the cell, LDs were classified as clustered. LDs were classified as intermediate when at least 50% of the LDs showed a dispersed distribution, and dispersed when LD distribution was undistinguishable from that non-transfected neighboring cells. Experiments were performed a minimum of three times.

Lysophosphatidylcholine hydrolase assays

At 48-h post-transfection, COS-7 cells were sonicated in 0.25 M sucrose, 1 mM EDTA, 1 mM DTT containing 20 μg/ml leupeptine, 2 μg/ml antipain, and 1 μg/ml pepstatin, and then centrifuged at 4°C and 1,000*g* to prepare protein samples. Protein concentrations were determined by BCA Protein Assay Kit using BSA as standard. The supernatant fraction was used to determine lysophospholipase activity as described previously (Heier et al., 2017). In brief, 50 μl cell lysates containing 50 μg of protein were incubated with a 50 μl substrate volume containing 4 mM LPC, 100 mM Bis-tris propane buffer, pH 8.0, 1 mM EDTA, and 4 mM CHAPS for 30 min at 37°C in a water bath. Each reaction was terminated by heat inactivation at 75°C for 10 min. The released amounts of fatty acids were determined using an HR Series NEFA-HR (2) kit according to the manufacturer's protocol.

Statistical analysis

All measurements were performed in triplicates. Data are presented as mean ± SD. Statistical significance was determined by the Student's unpaired *t*-test. Group differences were considered statistically significant for $P < 0.05$. Data analysis were carried out using SPSS 17.0 (IBM, USA).

RESULTS

The PNPLA7-C localizes to LDs *ex vivo* and associates with pre-existing LDs after starvation

Our previous study demonstrates that PNPLA7 associates with LDs via its C-region in COS-7 cells after OA loading (Heier et al., 2017). However, in the current study, we found that PNPLA7-C labeled vesicles appear as ring structures in some cells 48-h post-transfection without OA stimulation, although most of PNPLA7-C exhibits a diffused cytosolic distribution (Fig. 1B). The ring-like distribution of PNPLA7-C concentrates around LDs stained with a neutral lipid dye, LipidTOX Red (Fig. 1B), indicating that PNPLA7-C associates with LDs. This phenomena becomes more obvious and LD clustering appears 72-h post-transfection (Fig. 1B). Thus, PNPLA7-C localizes to LDs even under normal culture conditions without elevated fatty acid fluxes.

LD formation originates from pre-existing LD (pre-LD) in restricted ER microdomains (Kassan et al., 2013). Neutral lipids are first deposited in pre-LDs to stimulate LD formation upon fatty acids feeding. Pre-LDs are characterized with a core of neutral lipids that are resistant to starvation and can be labeled with a modeled peptide (HPos) after starvation

(Kassan et al., 2013). The relationship of PNPLA7 with pre-LDs was investigated to further explore the relationship between PNPLA7 and LDs. As shown in Fig. 1C, HPos fused with mCherry distributes in ER-like structures and associates with small dots (pre-LDs) after starvation. GFP with a diffused distribution is an HPos negative cell (Fig. 1C). There were a large number of small puncta in PNPLA7-C-GFP-expressing cells, most of which were HPos positive (Fig. 1C). In contrast to PNPLA7-C, PNPLA7 does not colocalize with pre-LDs labeled by HPos-mCherry, yet still exhibits a reticular staining pattern (Fig. 1C). Quantified analyses of our results indicate the percentage of HPos-positive small puncta in PNPLA7-C expressing cells is significantly increased when compared with PNPLA7 expressing cells (Fig. 1D). These data demonstrate that PNPLA7-C localizes to pre-LDs, as defined by HPos labeling, after starvation.

PNPLA7-C induces LD clustering in a non-enzymatic manner

The C-terminal region of PNPLA7 localizes to pre-LDs and mature LDs. We further examined the effect of PNPLA7 and its truncated mutants on LD distribution. As shown in Fig. 2, COS-7 cells overexpressing PNPLA7-C have LD clustering in proximity to the cell nucleus when compared with neighboring non-transfected cells and cells transfected with the empty vector GFP. In contrast, LDs in PNPLA7-expressing cells are relatively dispersed in the cytosol and most PNPLA7 does not localize to LDs, suggesting that LD targeting is necessary for LDs clustering. Elevated cAMP levels enhances the localization of PNPLA7 to LDs after fatty acid flux (Heier et al., 2017). Localization of PNPLA7 to LDs under increased cAMP conditions causes some LD clustering; however, most LDs are still dispersed in the cytosol (Fig. 2). PNPLA7 where regulatory(R-) region is deleted also localizes to LDs (Heier et al., 2017). There were less clustered and more dispersed LDs in PNPLA7-ΔR expressing cells compared with PNPLA7-C expressing cells (Fig. 2). Because PNPLA7-C and PNPLA7-ΔR exhibit the similar catalytic activity (Heier et al., 2017), the distribution of LDs induced by PNPLA7-C does not appear to be related to catalytic activity.

The entire putative TMD of PNPLA7-C is required for targeting LDs

In eukaryotes, *de novo* formation of LDs originates from the ER (Fujimoto et al., 2008). In addition, the patatin domain of human NTE may mediate the association of NTE's catalytic region with ER membranes (Wijeyesakere et al., 2007). These data suggest that the patatin domain of PNPLA7-C may also medicate its targeting to LDs. However, our previous results demonstrate that a PNPLA7 truncated mutant PNPLA7-C2, which only has a partial patatin domain, still localizes to LDs (Fig. 3A), strongly suggesting that the patatin domain is dispensable for LD targeting (Heier et al., 2017). To further identify the precise LD targeting motif, the putative TMDs were analyzed by different algorithms, even though the C-region of PNPLA7 was previously reported not to comprise an integral transmembrane protein (Heier et al., 2017). As shown in Table 2, there are 0, 3, or 4 putative TMDs in the PNPLA7-C as predicted by different algorithms. These putative TMDs are

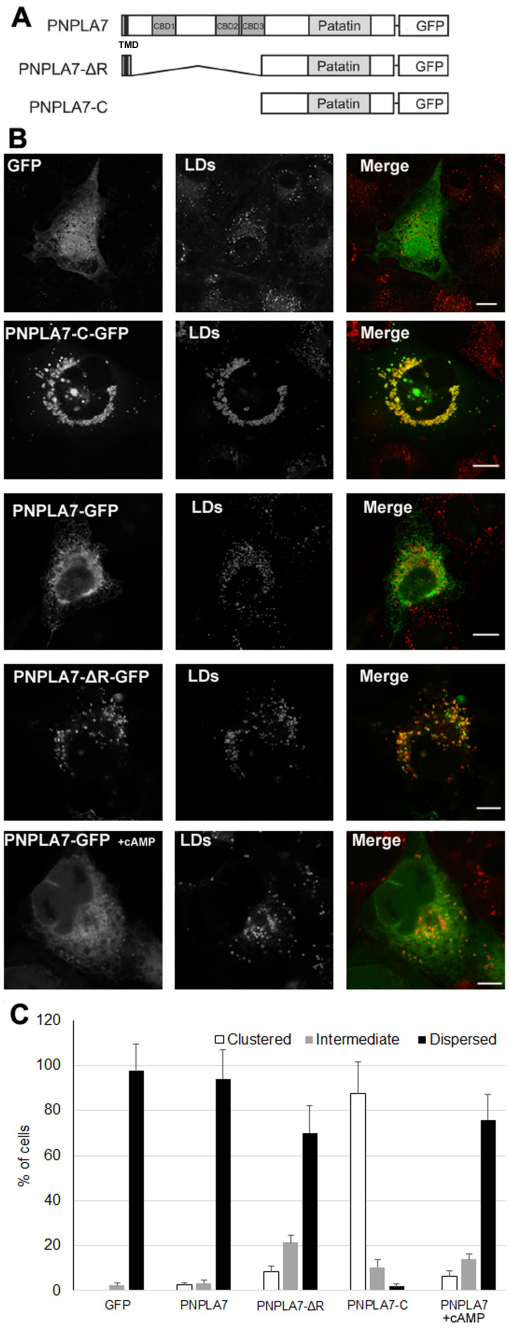

Fig. 2. PNPLA7-C induces LDs clustering. (A) Domain architecture of PNPLA7 variant used in these experiments. (B) Subcellular distribution of PNPLA7 variants and LDs. COS7 cells transiently expressing GFP, PNPLA7, and its variants were lipid-loaded for 16 h with 400 μM OA complexed to albumin and then fixed. PNPLA7-expressing cells were treated with 400 μM OA and 1 mM 8-CPT-cAMP for 16 h and then fixed. LD was stained with LipidTOX Red. Colocalization of proteins and LDs were visualized by confocal laser scanning microscopy. Scale bars = 10 μm. (C) Transfected cells with GFP, PNPLA7, and its variants were classified according to the distribution of their LDs. Results are given as mean ± SD from three independent experiments (60 cells were quantified in each condition).

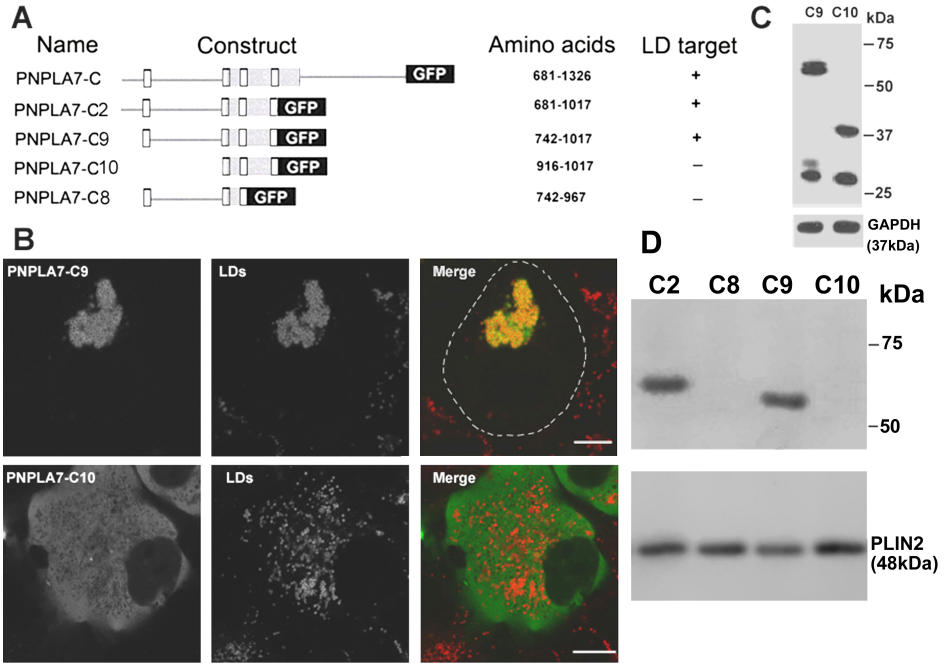

Fig. 3. The putative four TMDs of PNPLA7-C directs cytosolic GFP to LDs. (A) Schematic diagram of PNPLA7-C truncation mutants and their colocalization with LDs. A "+" indicates the detection of mutated PNPLA7-C on LDs; a "-" indicates the failure to detect the protein on LDs. (B) Subcellular distribution of PNPLA7-C truncation mutants and LDs. COS-7 transiently expressing GFP fused to various PNPLA7-C were incubated with 400 μM OA overnight and then fixed. LD was stained with LipidTOX Red. Colocalization of various PNPLA7-C-GFP constructs and LDs were visualized by confocal fluorescence microscopy. The discontinuous short white lines indicate cell boundaries. Scale bars = 10 μm. (C and D) The expression of PNPLA7-C truncation mutants in whole cell lysis and LD fractions were detected by immunoblotting using GFP antibody. The expression of GAPDH and PLIN2 were used as loading controls.

Table 2. Predicted transmembrane domains for murine PNPLA7-C

Analysis software	No. of TMDs	Location of TMD
TMHMM	0	
SOSUI	0	
TMpred	3	742-764, 916-935, 947-967
HMMTOP	3	916-935, 948-967, 998-1017
TopPred	4	741-761, 913-933, 948-968, 996-1016

common hydrophobic sequences that may associate with LD surface membranes.

When the stretch of residues 681-1017 (PNPLA7-C2) was further shortened to residues 742-1017 (PNPLA7-C9), which contains all four putative TMDs, PNPLA7-C9 was still sufficient for cytosolic GFP targeting to LDs (Figs. 3A and 3B). However, further N- or C-terminal truncations, PNLA7-C8 and PNPLA7-C10 which delete the first and fourth TMD respectively, do not localize to LDs (Figs. 3A and 3B) (Heier et al., 2017). To further confirm the interactions of PNPLA7 truncated mutants with LDs, we fractionated transfected COS-7 cells by ultracentrifugation and assessed the abundance of each PNPLA7 mutant in the LD fraction by immunoblotting analysis. As shown in Figs. 3C and 3D, ectopically expressed PNPLA7-C2 and C9, but not C8 and C10, are markedly enriched in the LD fraction resembling the distribution of the endogenous LD protein (PLIN2) consistent with our microscopy data. These results indicate that the entire putative TMD functions as the LD targeting motif. To further confirm these results, a mutant lacking the entire putative TMDs (ΔTM-PNPLA7-C) was constructed. ΔTM-PNPLA7-C evenly distributes in the cytoplasm and does not localize with LDs (Fig. 4). Thus, amino acids 742-1017 containing up to four putative TMDs is required for the localization of PNPLA7-C to LDs.

The carboxyl-terminal region of PNPLA7-C blocks LD targeting

We further investigated the role of the C-terminal region of PNPLA7-C in LD targeting. A truncated mutant, PNPLA7-C5 (aa 742-1326), does not localize to LDs, although it contains the entire putative TMDs; indicated that the C-terminal region has an anti-LDs targeting effect (Fig. 5A) (Heier et al., 2017). Another C-terminal truncation, PNPLA7-C11 (aa 742-1207) is distributed in cytoplasm as well and does not localize on LD surfaces (Fig. 5B). In contrast, a C-terminal truncation, PNPLA7-C12 (aa 742-1168) localizes to LDs (Fig. 5B). The expression of PNPLA7-C truncated mutants in the LD fraction further confirms that PNPLA7-C12, but not PNPLA7-C5 or -C11 associate with LDs (Figs. 5C and 5D). These results demonstrate that the C-terminal region of PNPLA7-C, at least residues 1169-1326, block LD targeting.

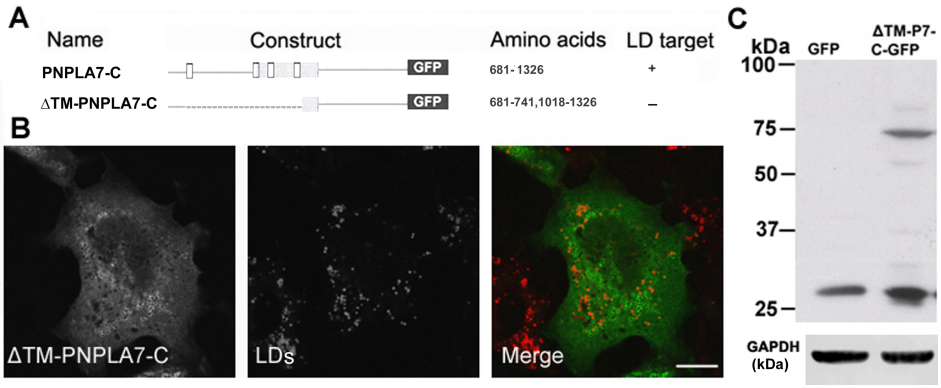

Fig. 4. The entire putative TMD is required for the localization of PNPLA7-C to LDs. (A) Schematic overview of PNPLA7-C lacking the entire putative TMD (ΔTM-PNPLA7-C) and its association with LDs. A "-" indicates the failure to detect the protein on LDs while a "+" shows the association with LDs. (B) Subcellular distribution of ΔTM-PNPLA7-C-GFP in COS-7 cells. Formation of LDs was induced by incubation with FA, and the subcellular localization of the recombinant protein was assessed by confocal fluorescence microscopy. LDs were visualized using HSC LipidTOX Deep Red. Scale bar = 10 μm. (C) The expression of ΔTM-PNPLA7-C-GFP mutants in whole cell lysis were analyzed by immunoblotting using GFP antibody.

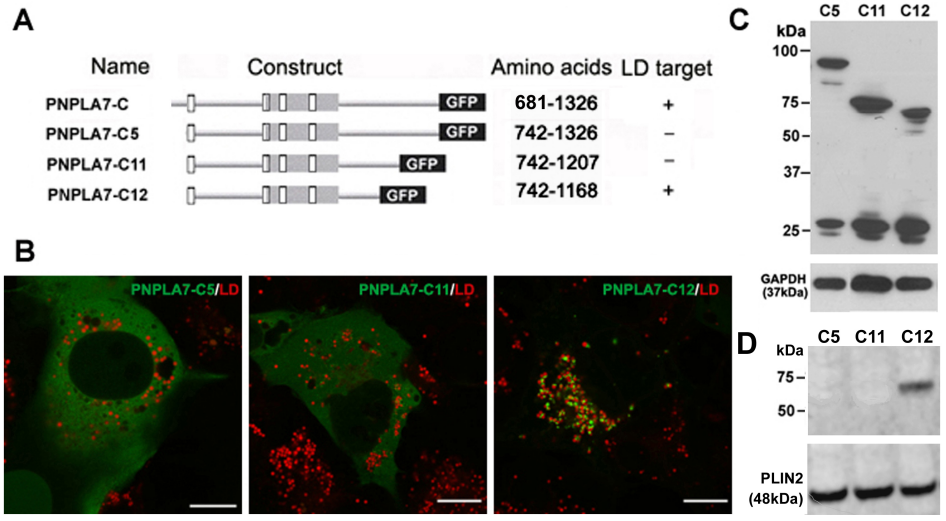

Fig. 5. The carboxyl-terminal region of PNPLA7-C blocks LD targeting. (A) Schematic diagram of C-terminal truncation mutants of PNPLA7-C and their colocalization with LDs. Disassociation with LDs is described as negative (-) and localization to LDs as positive (+). (B) Subcellular localization of C-terminal truncated mutants in COS-7 cells. Various PNPLA7-C mutants tagged with GFP were expressed and LDs were induced by 400 μM OA loading for 16 h. LDs was stained with LipidTOX Red. Colocalization of various PNPLA7-C-GFP constructs and the LDs were visualized by confocal fluorescence microscopy. Scale bars = 10 μm. (C and D) The abundance of proteins in whole cellular extracts and LD fractions were assessed by immunoblotting analysis using antibodies against GFP, GAPDH, and PLIN2.

The N-terminal region of PNPLA7-C contributes to LD targeting

PNPLA7-C2 containing the N-terminal sequence and the entire putative TMDs localizes to LDs, suggesting that the N-terminal residues 681-741 do not block LD targeting like the C-terminal region (Heier et al., 2017). However, the role of N-terminal residues 681-741 in the LD targeting is unknown. When the fourth putative TMD was deleted, PNPLA7-C3 (aa 681-967 containing the N-terminal region and the first to third putative TMDs) localizes to LDs; which as unexpected (Fig. 6B). However, a shorter C-terminal mutant, PNPLA7-C4, lacking both the third and the fourth putative TMDs, does not localize to LDs. However, the mutant PNPLA7-C13 where the second TMD was deleted in PNPLA7-C3 does localize to LDs (Fig. 6B). In contrast, further deletion of the N-terminal region in PNPLA7-C13 resulted in the failure to detect LD association (Fig. 6B). The localizations of PNPLA7 truncated mutants to LDs were further verified by immunoblotting analysis in the LD fraction (Figs. 6C and 6D). These results are summed in Fig. 6A and indicate that the N-terminal of PNPLA7-C2 contributes to LD targeting, independent of the second and fourth putative TMD.

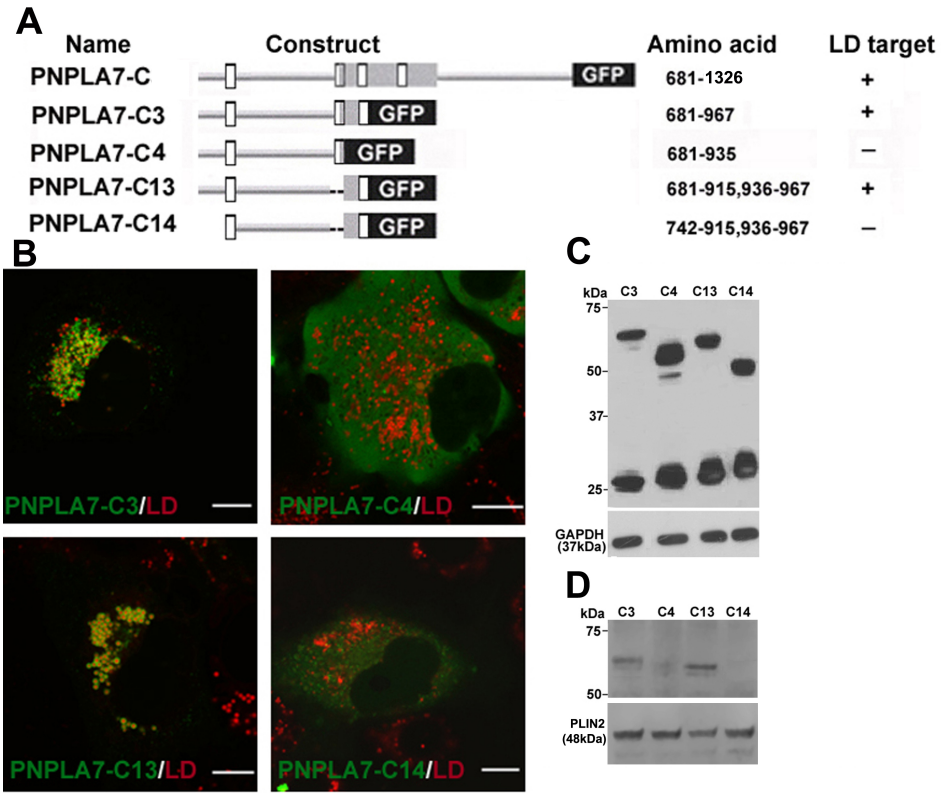

Fig. 6. The N-terminal region of PNPLA7-C, amino acids 681-741, contributes to LD targeting. (A) Schematic diagram of PNPLA7-C mutants tagged with GFP and their colocalization with LD. Mutants failing to localize to LDs were described as negative (-). Those labeled "+" localize to LDs. (B) Subcellular distribution of PNPLA7-C variants. COS-7 were transfected with various PNPLA7-C mutants and LDs were induced by OA loading for 16 h and then fixed. LipidTOX Red was used to stain LDs. Colocalization of various PNPLA7-C-GFP constructs and LDs were visualized by confocal laser scanning microscopy. Scale bars = 10 μm. (C and D) The expression of PNPLA7-C truncation mutants in whole cellular lysates and LD fractions was detected by immunoblotting using GFP antibody. The GAPDH and PLIN2 were used as loading controls.

The LD targeting motif of PNPLA7-C does not exhibit catalytic activity

Both PNPLA7 and PNPLA7-C have lysophospholipase activity and hydrolyze LPC *in vivo* (Heier et al., 2017). The catalytic activity of PNPLA7 needs membrane associations with both the ER and LDs (Heier et al., 2017). We assayed the catalytic activity the LD targeting motif and contribution stretch of the PNPLA7-C after OA loading. As shown in Fig. 7, compared to GFP controls, PNPLA7 and PNPLA7-C significantly increase LPC hydrolase activity. In contrast, PNPLA7-C9 containing the LD targeting motif and PNPLA7-C2 including the N-terminal stretch and LD targeting motif have similar lysophospholipase activities with GFP controls. Thus, the LD targeting motif of PNPLA7 does not exhibit catalytic activity, although it localizes on LDs surface membranes.

DISCUSSION

How proteins target LDs is a major question in LD biology. Protein-lipid direct interactions of LD proteins are a primary foci, although the targeting of proteins to LDs can also be achieved by proteins interacting with other LD proteins. As an LPC hydrolase, PNPLA7 is associated with LDs directly through its C-terminal region after fatty acid loading and cyclic nucleotide stimulation (Heier et al., 2017). In this study, the interaction of PNPLA7 with LDs through its C-terminal region was further characterized.

LD formation originates from pre-LDs in restricted ER microdomains (Kassan et al., 2013). After starvation, PNPLA7-C localization corresponds to pre-LDs as defined by HPos labeling, suggesting that PNPLA7-C may medicate the localization of PNPLA7 to pre-LDs. However, when compared to PNPLA7-C, the colocalization percentage of PNPLA7 with pre-LDs is reduced. This may be related to the existence of the R-region and the N-terminal putative TMDs. Our previous results showed that the N-terminal TMD anchored on the ER and the R-region inhibited the association of PNPLA7-C with LDs after fatty acids loading (Heier et al., 2017). Localization of PNPLA7 to LDs is enhanced by elevated cAMP analogues (Heier et al., 2017). Thus, the interaction of PNPLA7 with pre-LDs may be dependent on the cyclic nucleotides, such as cAMP and cGMP.

A variety of mechanisms have evolved to target proteins to LDs. In general, there are two major pathways; from the ER or from the cytosol (Kory et al., 2016). Although PNPLA7 is an ER-anchored protein via its N-terminal TMD and is

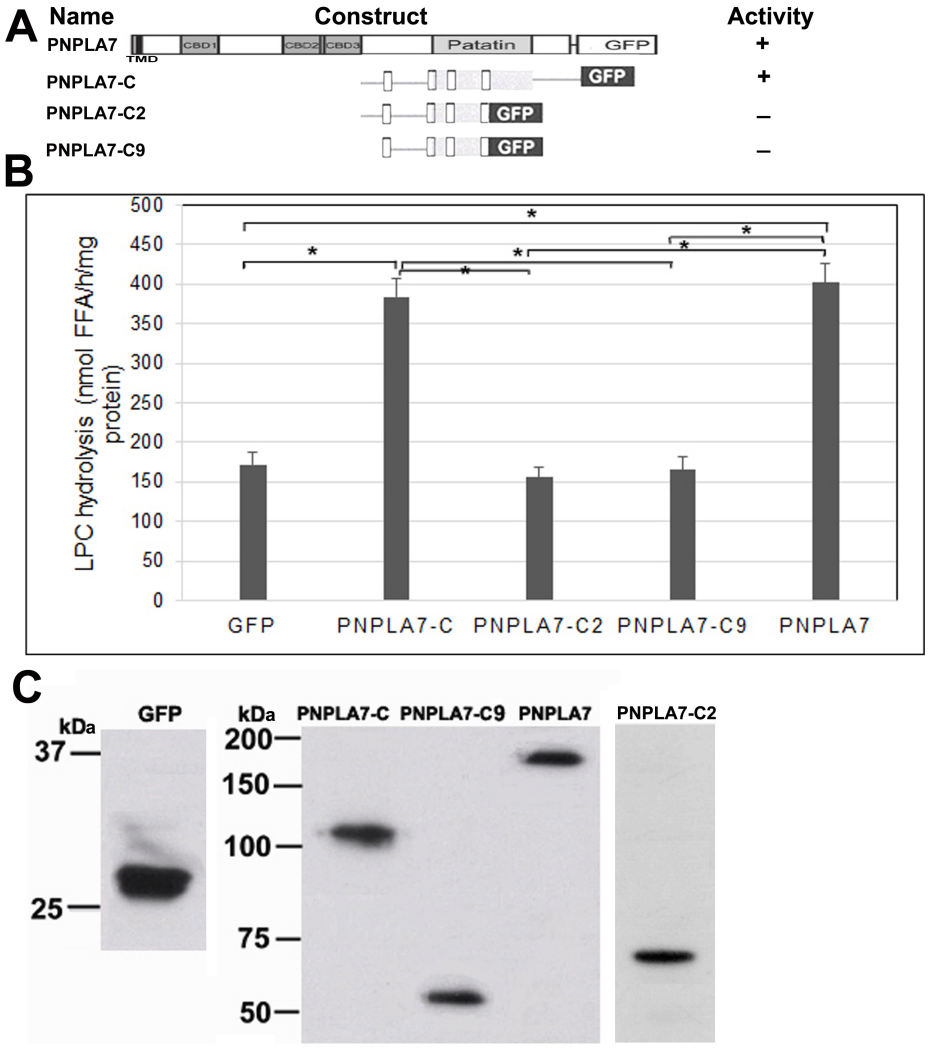

Fig. 7. The LPC hydrolase activity of PNPLA7, PNPLA7-C, and LD targeting motif. (A) Schematic diagram of PNPLA7 and its truncated mutants tagged with GFP and their catalytic activities. Mutants exhibiting LPC hydrolase activity were described as positive (+), otherwise as negative (-). (B) LPC hydrolase activities of PNPLA7 and truncated mutants. COS-7 transiently expressing PNPLA7, PNPLA7-C, PNPLA7-C2, and PNPLA7-C9 fused with GFP were incubated with 400 μM OA for 16 h and then assayed LPC hydrolase activity. Following, the nucleus soluble (PNS) fraction was incubated with C18:1 LPC as a substrate and the release of free fatty acids (FFAs) was determined. LPC hydrolase activity is presented as the released FFAs. Data are representative of two independent experiments and are expressed as a mean (n = 3). Error bars represent SD. Statistical significance was determined using Student's unpaired *t*-test. $*P < 0.05$. (C) Protein levels of PNPLA7 variants in COS-7 cells. Cells were transfected with PNPLA7-GFP or truncated mutants and protein levels were analyzed in PNSs by immunoblotting analysis using an antibody against GFP.

associated with LDs after cyclic nucleotides stimulation, the N-terminus is still anchored on the ER membrane while the C-terminal regions localizes to LDs (Heier et al., 2017). PNPLA7-C is not an integral transmembrane protein, although fragments of PNPLA7-C associate with the ER membrane as displayed by subcellular fractionation immunoblotting analyses (Heier et al., 2017). Thus, both PNPLA7 and PNPLA7-C belong to "class II" proteins that translocate from cytosol to LDs, although PNPLA7 is an ER-anchored protein.

The localization of most class II proteins to LD surfaces is through amphipathic helices or via multiple amphipathic and hydrophobic helices, which are distinct, non-exclusive targeting mechanisms (Kory et al., 2016). The sequence of PNPLA6 patatin domains have been proposed to be amphipathic and unfolded in solution, but fold into a helix when binding a membrane surface (Wijeyesakere et al., 2007). A model for this amphipathic helix suggests that the C-region of PNPLA6 associates with the ER bilayer membranes through the PNPLA6 patatin domain (Wijeyesakere et al., 2007). Thus, these amphipathic helices might interact with LD surfaces in a manner similar to the ER such that the hydrophilic residues face the aqueous phase and interact with the polar head groups of the phospholipids, with the hydrophobic surface being embedded in the acyl-chain domain of the LD membrane

(Hristova et al., 2009; Seelig, 2004). However, although there is a high similarity between the patatin sequences of PNPLA6 and PNPLA7, the patatin domain was largely dispensable for LD targeting (Heier et al., 2017). TMD analysis indicates that there are 0-4 putative TMDs in PNPLA7-C (Table 2). By generating PNPL7-C mutants, we found that these putative TMDs were sufficient for LD targeting and are required for the localization of PNPLA7-C to LDs. The identified LD targeting motif is shorter than the previously identified region (Heier et al., 2017). Thus, the interaction of PNPLA7-C with LDs is dependent on multiple hydrophobic helices found in transmembrane helices, which differ from amphipathic helices in that all their residues tend to form hydrophobic helices. Mutated PNPLA7-C lacking the first or fourth TMD showed reduced LD targeting, indicating both the first and the fourth TMD are required for LD targeting.

Although the entire putative transmembrane region is associated with LDs after lipid loading, it does not exhibit any LPC hydrolase activity like PNPLA7 and PNPLA7-C, because the LD targeting motif does not contain the whole patatin domain. There are three essential activity sites, Asp960, Ser 966, and Asp1086 in the patatin domain of PNPLA6 (Atkins and Glynn, 2000; Wijeyesakere et al., 2007). Compared with PNPLA6, Asp951, Ser957 and Asp1077 may constitute a catalytic triplet in the patatin domain of PNPLA7. The LD targeting motif does not contain the essential Asp1077 in the active site. These results indicate that the LD targeting motif is distinct from the catalytic activity domain in PNPLA7.

Although the central residues (residues 742-1016) contain four putative TMDs required for the LD targeting of PNPLA7-C, the flanking sequences may also influence the proper hydrophobic helix packing required for LD targeting. This is true of other LD proteins as well, such as caveolin-1 and oleosins (Ostermeyer et al., 2004; Tzen et al., 1992). Our findings indicate that the N-terminal flanking sequence, residues 681-741, contribute to the LD targeting. When the N-terminal flanking sequence is present, a mutant lacking both the second and the fourth putative TMD still localizes to LDs. A Gly-Ala-rich face was found in the helix formed by the first half of the hydrophobic domain of caveolin-1 (Ostermeyer et al., 2004). Similarly, Gly, Ala, and Ser that prefer to be at contact sites between membrane-embedded helices are unusually rich in the N-terminal half of oleosins hydrophobic domains (Tzen et al., 1992). Gly, Ala, and Ser comprise over 30% of the N-terminal flanking sequence in the LD targeting motif of PNPLA7-C (data not shown). Lipid-embedded helices generally pack more tightly than helices in soluble proteins (Eilers et al., 2000). Thus we speculate that the N-terminal flanking sequence of PNPLA7-C may contribute to tighter packing of the central hydrophobic putative TMDs. In contrast, the C-terminal flanking sequence contains fewer Gly, Ala, and Ser residues. Hydrophobic and hydrophilic analysis of PNPLA7-C indicate hydrophilic properties for the C-terminal sequence (data not shown). Thus the C-terminal flanking sequence from residue 1169 to the end of the protein blocks LD targeting.

Overexpression of PNPLA7-C induces LD clustering that is dependent on LD targeting, not enzymatic activity. How do the catalytic domains of PNPLA7 cause LDs clustering? Changes in the ER morphology induced by PNPLA6, PNPLA7, and their truncated mutants may provide some clues (Heier et al., 2017; Li et al., 2003). PNPLA6 and PNPLA7 are anchored on the ER via the N-terminal TMD, and their overexpression causes ER aggregation through the intermolecular association of C-terminal domains, which is hindered by the R-region to some degree (Heier et al., 2017; Li et al., 2003). Thus, when LDs formation is induced by FA loading, PNPLA7-C localizes to LDs and the intermolecular association of PNPLA7-C leads to LD clustering which is not related to catalytic activity. The R-region hinders the localization of the C-terminal domain to LDs and causes the disassociation of PNPLA7 with LDs as shown in Fig. 2. In addition, when the R-region is deleted, the C-terminal domain localizes to LDs and results in less clustered and more dispersed LDs than PNPLA7-C, which may be related to the N-terminal TMD anchored to the ER membrane; this interaction may block the intermolecular association of C-terminal domains.

In summary, our findings characterize the specific functional domains of PNPLA7 the mediate subcellular positioning and interactions with LDs. The interaction of PNPLA7 through its catalytic region with LDs was characterized for the first time as displayed in Fig. 8. The localization of PNPLA7 catalytic domains to LDs is dependent on a central region of residues 742-1016 which contains four putative TMDs. The N-terminal

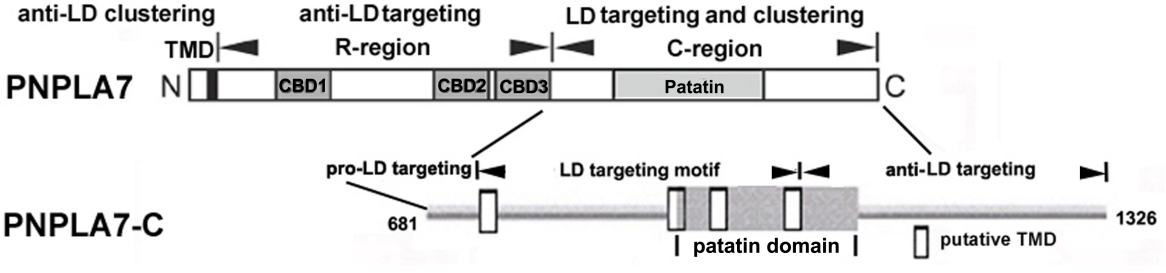

Fig. 8. The structural and functional domains of PNPLA7 interacted with LDs. PNPLA7 interacts with LDs through its C-terminal region. The C-terminus mediates LD localization and clustering, whereas the N-terminal putative TMD has anti-LD clustering and anti-LD localization activity. In the C-terminal region, a central region containing four putative TMDs functions as an LD targeting motif and is essential for the localization of PNPLA7-C to LDs. The N-terminal flanking region acts as a pro-LD targeting motif and contributes to the LD targeting, whereas the C-terminal region blocks LD localization as acts an anti-LD targeting motif. In addition, the patatin domain mediates the catalytic function of PNPLA7.

flanking region and C-terminal region contribute to and block the LD targeting respectively. The LD targeting motif with multiple hydrophobic helices is different from the catalytic domain containing the whole patatin domain. In addition, localization of PNPLA7-C induces LDs clustering through intermolecular associations in a non-enzymatic manner, which is hindered by the R-region and the N-terminal TMD to some degree. These findings provide critical insights into an evolutionarily conserved phospholipid-hydrolyzing enzymes family. The precise structure of PNPLA7-C needs to be further explored and will help the understanding of the structure and function of PNPLA7 interactions with the ER and LDs.

Disclosure

The authors have no potential conflicts of interest to disclose.

ACKNOWLEDGMENTS

This work is supported by grants from the National Nature Science Foundation of China (No. 31801139 to F.H.), Chongqing Science and Technology Bureau (No. cstc2018jcyjAX0120 to P.C., cstc2016jcyjA0572 to F.H.) and Chongqing Entrepreneurship and Innovation Support Project for Returnees (to P.C.). We would like to thank Prof. Albert Pol (Institut d'Investigacions Biomèdiques August Pi i Sunyer (Barcelona, Spain) for providing pGFP-HPos plasmid and Prof. Rudolf Zechner (University of Graz, Austria) for supervision.

ORCID

Pingan Chang https://orcid.org/0000-0002-2244-1929
Tengteng Sun https://orcid.org/0000-0001-9042-6571
Christoph Heier https://orcid.org/0000-0001-6858-408X
Hao Gao https://orcid.org/0000-0002-1928-3296
Hongmei Xu https://orcid.org/0000-0002-3104-5493
Feifei Huang https://orcid.org/0000-0002-2109-307X

REFERENCES

Akassoglou, K., Malester, B., Xu, J., Tessarollo, L., Rosenbluth, J., and Chao, M.V. (2004). Brain-specific deletion of neuropathy target esterase/swisscheese results in neurodegeneration. Proc. Natl. Acad. Sci. U. S. A. *101*, 5075-5080.

Atkins, J. and Glynn, P. (2000). Membrane association of and critical residues in the catalytic domain of human neuropathy target esterase. J. Biol. Chem. *275*, 24477-24483.

Barneda, D. and Christian, M. (2017). Lipid droplet growth: regulation of a dynamic organelle. Curr. Opin. Cell Biol. *47*, 9-15.

Brasaemle, D.L. and Wolins, N.E. (2016). Isolation of lipid droplets from cells by density gradient centrifugation. Curr. Protoc. Cell Biol. *72*, 3.15.1-3.15.13.

Chang, P.A., Wang, Z.X., Long, D.X., Qin, W.Z., Wei, C.Y., and Wu, Y.J. (2012). Identification of two novel splicing variants of murine NTE-related esterase. Gene *497*, 164-171.

Claros, M.G. and von Heijne, G. (1994). TopPred II: an improved software for membrane protein structure predictions. Comput. Appl. Biosci. *10*, 685-686.

Eilers, M., Shekar, S.C., Shieh, T., Smith, S.O., and Fleming, P.J. (2000). Internal packing of helical membrane proteins. Proc. Natl. Acad. Sci. U. S. A. *97*, 5796-5801.

Farese, R.V., Jr. and Walther, T.C. (2009). Lipid droplets finally get a little R-E-S-P-E-C-T. Cell *139*, 855-860.

Fujimoto, T., Ohsaki, Y., Cheng, J., Suzuki, M., and Shinohara, Y. (2008). Lipid droplets: a classic organelle with new outfits. Histochem. Cell Biol. *130*, 263-279.

Fujimoto, T. and Parton, R.G. (2011). Not just fat: the structure and function of the lipid droplet. Cold Spring Harb. Perspect. Biol. *3*, a004838.

Heier, C., Kien, B., Huang, F., Eichmann T.O., Xie, H., Zechner, R., and Chang, P.A. (2017). The phospholipase PNPLA7 functions as a lysophosphatidylcholine hydrolase and interacts with lipid droplets through its catalytic domain. J. Biol. Chem. *292*, 19087-19098.

Hirokawa, T., Boon-Chieng, S., and Mitaku, S. (1998). SOSUI: classification and secondary structure prediction system for membrane proteins. Bioinformatics *14*, 378-379.

Hofmann, K. and Stoffel, W. (1993). TMbase - a database of membrane spanning proteins segments. Biol. Chem. Hoppe-Seyler *374*, 166.

Hristova, K., Wimley, W.C., Mishra, V.K., Anantharamiah, G.M., Segrest, J.P., and White, S.H. (2009). An amphipathic alpha-helix at a membrane interface: a structural study using a novel X-ray diffraction method. J. Mol. Biol. *290*, 99-117.

Huang, F.F., Chang, P.A., Sun, L.X., Qin, W.Z., Han, L.P., and Chen, R. (2016). The destruction box is involved in the degradation of the NTE family proteins by the proteasome. Mol. Biol. Rep. *43*, 1285-1292.

Kassan, A., Herms, A., Fernández-Vidal, A., Bosch, M., Schieber, N.L., Reddy, B.J., Fajardo, A., Gelabert-Baldrich, M., Tebar, F., Enrich, C., et al. (2013). Acyl-CoA synthetase 3 promotes lipid droplet biogenesis in ER microdomains. J. Cell Biol. *203*, 985-1001.

Kien, B., Grond, S., Haemmerle, G., Lass, A., Eichmann, T.O., and Radner, F.P.W. (2018). ABHD5 stimulates PNPLA1-mediated ω-*O*-acylceramide biosynthesis essential for a functional skin permeability barrier. J. Lipid Res. *59*, 2360-2367.

Kienesberger, P.C., Lass, A., Preiss-Landl, K., Wolinski, H., Kohlwein, S.D., Zimmermann, R., and Zechner, R. (2008). Identification of an insulin-regulated lysophospholipase with homology to neuropathy target esterase. J. Biol. Chem. *283*, 5908-5917.

Kienesberger, P.C., Oberer, M., Lass, A., and Zechner, R. (2009). Mammalian patatin domain containing proteins: a family with diverse lipolytic activities involved in multiple biological functions. J. Lipid Res. *50* Suppl, S63-S68.

Kory, N., Farese, R.V., Jr., and Walther, T.C. (2016). Targeting fat: mechanisms of protein localization to lipid droplets. Trends Cell Biol. *26*, 535-546.

Krogh, A., Larsson, B., von Heijne, G., and Sonnhammer, E.L. (2001). Predicting transmembrane protein topology with a hidden Markov model: application to complete genomes. J. Mol. Biol. *305*, 567-580.

Li, Y., Dinsdale, D., and Glynn, P. (2003). Protein domains, catalytic activity, and subcellular distribution of neuropathy target esterase in Mammalian cells. J. Biol. Chem. *278*, 8820-8825.

Lush, M.J., Li, Y., Read, D.J., Willis, A.C., and Glynn, P. (1998). Neuropathy target esterase and a homologous Drosophila neurodegeneration-associated mutant protein contain a novel domain conserved from bacteria to man. Biochem. J. *332*(Pt 1), 1-4.

Murugesan, S., Goldberg, E.B., Dou, E., and Brown, W.J. (2013). Identification of diverse lipid droplet targeting motifs in the PNPLA family of triglyceride lipases. PLoS One *8*, e64950.

Ohno, Y., Nara, A., Nakamichi, S., and Kihara, A. (2018). Molecular mechanism of the ichthyosis pathology of Chanarin-Dorfman syndrome: Stimulation of PNPLA1-catalyzed ω-O-acylceramide production by ABHD5. J. Dermatol. Sci. *92*, 245-253.

Ostermeyer, A.G., Ramcharan, L.T., Zeng, Y., Lublin, D.M., and Brown, D.A. (2004). Role of the hydrophobic domain in targeting caveolin-1 to lipid droplets. J. Cell Biol. *164*, 69-78.

Papadopoulos, C., Orso, G., Mancuso, G., Herholz, M., Gumeni, S., Tadepalle, N., Jüngst, C., Tzschichholz, A., Schauss, A., Höning, S., et al. (2015). Spastin binds to lipid droplets and affects lipid metabolism. PLoS

Genet. *11*, e1005149.

Pichery, M., Huchenq, A., Sandhoff, R., Severino-Freire, M., Zaafouri, S., Opálka, L., Levade, T., Soldan, V., Bertrand-Michel, J., Lhuillier, E., et al. (2017). PNPLA1 defects in patients with autosomal recessive congenital ichthyosis and KO mice sustain PNPLA1 irreplaceable function in epidermal omega-O-acylceramide synthesis and skin permeability barrier. Hum. Mol. Genet. *26*, 1787-1800.

Quistad, G.B., Barlow, C., Winrow, C.J., Sparks, S.E., and Casida, J.E. (2003). Evidence that mouse brain neuropathy target esterase is a lysophospholipase. Proc. Natl. Acad. Sci. U. S. A. *100*, 7983-7987.

Read, D.J., Li, Y., Chao, M.V., Cavanagh, J.B., and Glynn, P. (2009). Neuropathy target esterase is required for adult vertebrate axon maintenance. J. Neurosci. *29*, 11594-11600.

Reue, K. (2011). Lipid droplet storage and metabolism: from yeast to man. J. Lipid Res. *52*, 1865-1868.

Seelig, J. (2004). Thermodynamics of lipid-peptide interactions. Biochim. Biophys. Acta *1666*, 40-50.

Sztalryd, C. and Brasaemle, D.L. (2017). The perilipin family of lipid droplet proteins: Gatekeepers of intracellular lipolysis. Biochim. Biophys. Acta Mol. Cell Biol. Lipids *1862*, 1221-1232.

Tusnády, G.E. and Simon, I. (2001). The HMMTOP transmembrane topology prediction server. Bioinformatics *17*, 849-850.

Tzen, J.T., Lie, G.C., and Huang, A.H. (1992). Characterization of the charged components and their topology on the surface of plant seed oil bodies. J. Biol. Chem. *267*, 15626-15634.

van Tienhoven, M., Atkins, J., Li, Y., and Glynn, P. (2002). Human neuropathy target esterase catalyzes hydrolysis of membrane lipids. J. Biol. Chem. *277*, 20942-20948.

Wijeyesakere, S.J., Richardson, R.J., and Stuckey, J.A. (2007). Modeling the tertiary structure of the patatin domain of neuropathy target esterase. Protein J. *26*, 165-172.

Wilson, P.A., Gardner, S.D., Lambie, N.M., Commans, S.A., and Crowther, D.J. (2006). Characterization of the human patatin-like phospholipase family. J. Lipid Res. *47*, 1940-1949.

Zaccheo, O., Dinsdale, D., Meacock, P.A., and Glynn, P. (2004). Neuropathy target esterase and its yeast homologue degrade phosphatidylcholine to glycerophosphocholine in living cells. J. Biol. Chem. *279*, 24024-24033.

Zhang, C. and Liu, P. (2019). The new face of the lipid droplet: lipid droplet proteins. Proteomics *19*, e1700223.